AECL-7161

ATOMIC ENERGY OF CANADA LIMITED

L'ÉNERGIE ATOMIQUE DU CANADA LIMITÉE

INITIAL FIELD MEASUREMENTS ON THE CHALK RIVER SUPERCONDUCTING CYCLOTRON

Mesures initiales du champ magnétique du cyclotron supraconducteur de Chalk River

J.H. ORMROD, K.C. CHAN and J.H. HILL

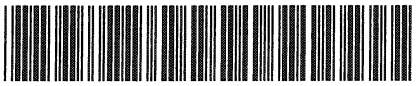

Chalk River Nuclear Laboratories Laboratoires nucléaires de Chalk River

Chalk River, Ontario

December 1980 décembre

ATOMIC ENERGY OF CANADA LIMITED

INITIAL FIELD MEASUREMENTS ON THE CHALK RIVER SUPERCONDUCTING CYCLOTRON

J.H. Ormrod, K.C. Chan and J.H. Hill

Research Company
Physics Division, Chalk River Nuclear Laboratories
Chalk River, Ontario K0J 1J0

December 1980

AECL-7161

L'ENERGIE ATOMIQUE DU CANADA, LIMITEE

Mesures initiales du champ magnétique du cyclotron supraconducteur de Chalk River

par

J.H. Ormrod, K.C. Chan et J.H. Hill

Résumé

Le champ magnétique sur plan médian du cyclotron supraconducteur de Chalk River a été mesuré en détail dans la gamme opérationnelle complète allant de 2.5 à 5 tesla. On décrit l'appareil de mesure du champ magnétique et on donne des résultats concernant la stabilité, la reproductibilité et le contenu harmonique de ce champ.

Société de recherche
Laboratoires nucléaires de Chalk River
Chalk River, Ontario KOJ 1JO

Décembre 1980

AECL-7161

ATOMIC ENERGY OF CANADA LIMITED

INITIAL FIELD MEASUREMENTS ON THE CHALK RIVER SUPERCONDUCTING CYCLOTRON

J.H. Ormrod, K.C. Chan and J.H. Hill

Abstract

The midplane magnetic field of the Chalk River superconducting cyclotron has been mapped in detail over the full operating range of 2.5 to 5 tesla. The field measuring apparatus is described and results given include measurements of the field stability, reproducibility and harmonic content.

Research Company
Physics Division, Chalk River Nuclear Laboratories
Chalk River, Ontario K0J 1J0

December 1980

AECL-7161

INITIAL FIELD MEASUREMENTS ON THE CHALK RIVER SUPERCONDUCTING CYCLOTRON

J.H. Ormrod, K.C. Chan and J.H. Hill

Atomic Energy of Canada Limited
Research Company
Physics Division, Chalk River Nuclear Laboratories
Chalk River, Ontario K0J 1J0

Introduction

The Chalk River superconducting heavy-ion cyclotron[1] is designed to accelerate all ions from lithium (to 50 MeV/nucleon) to uranium (to 10 MeV/nucleon).

Figure 1 shows a cutaway view of the mild steel magnet with the upper flutter poles omitted for clarity. It has four spiral sectors and the average induction at the midplane spans the range 2.5 to 5 T. The octagonal yoke is 3.36 m from flat to flat and the walls are 0.5 m thick. The overall height is 3.01 m and the midplane gap is 40 mm. The 300 mm diameter central holes in the poles accommodate the coaxial tuning lines for the radiofrequency accelerating system. The field measuring apparatus occupies the midplane gap and the lower central hole when the rf system is removed. Figure 2 shows the skirt and flutter poles in more detail.

The 6 MA turn superconducting coil is divided into inner and outer coil pairs of equal size as shown in Fig. 1. Coarse isochronization is achieved by adjusting the relative excitation of these coil pairs; the magnetic field is fine tuned by the use of movable iron trim rods[2]. In the final configuration, there are thirteen trim rods per hill. For the measurements reported here, all the holes were bored in

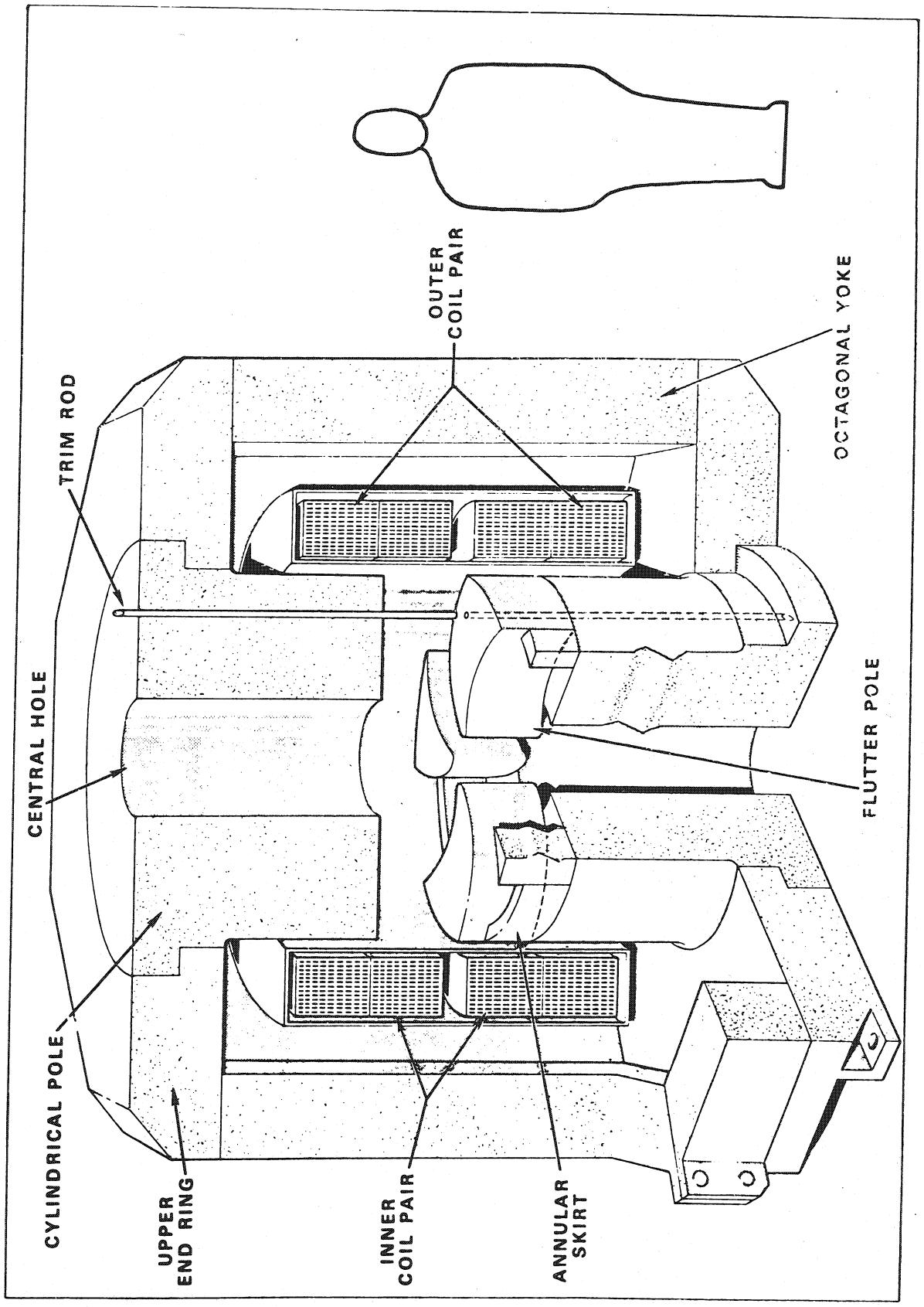

Fig. 1 Cutaway view of magnet. For clarity, the upper flutter poles are not shown.

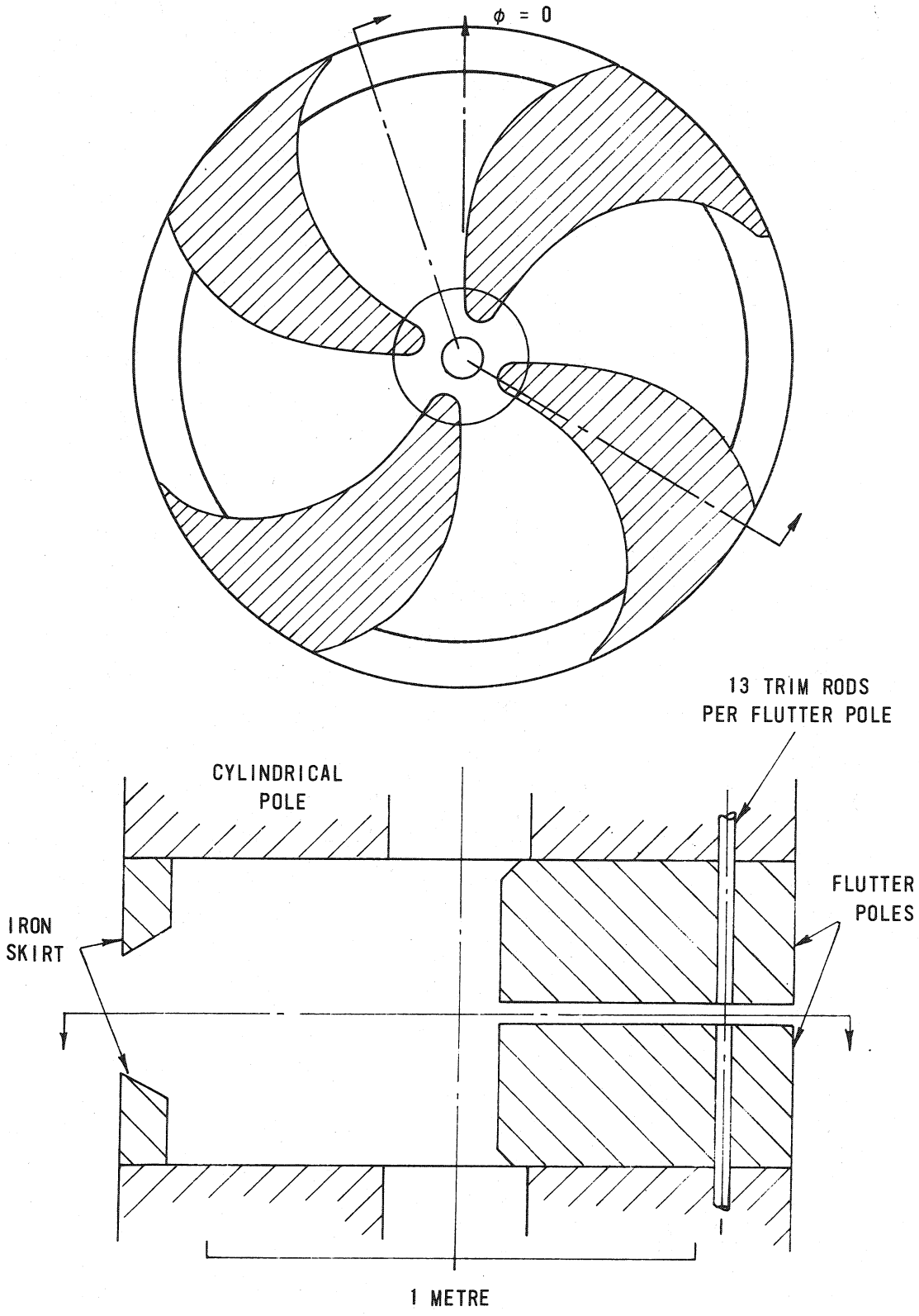

Fig. 2 Flutter pole assembly.

the cylindrical poles, but only three trim rod holes were bored through each flutter pole. Trim rods were inserted in these twenty-four completed holes, and the other eighty holes were empty from the outside of the yoke to the outside surface of the 100 mm thick flutter pole plate, i.e. to within 420 mm of the midplane. The effect of these holes in the poles is roughly a 60 mT reduction in the midplane field[3].

The magnetic field was measured using the flip-coil technique. The field measuring apparatus was designed to have the flip-coil arm replaceable by sets of diametrically opposed fixed coils that would sweep the midplane to measure the first harmonic component of the field. However, the reproducibility of the measurements with the flip-coils exceeded our expectations. The Fourier components were easily extracted from the raw field data, and the sweeping fixed coils were not used. Most of the measurements reported here were taken in late May and early June 1979 and represent the first detailed field mapping of the superconducting cyclotron. Using these data, modifications to the flutter poles were calculated which will reduce the trim rod amplitudes required to isochronize the wide range of ions to be accelerated. When these modifications are completed and all the trim rods installed, the field will be mapped again.

Field Measuring Apparatus

Figure 3 shows an isometric view of the field mapping apparatus. Forty flip-coils were distributed along an acrylic rod (the flip-coil arm) which was supported by a fibreglass structure and spanned the radial extent of the cyclotron poles. (The radial positions of the flip-coils are listed in Table I.) The section of the arm that holds

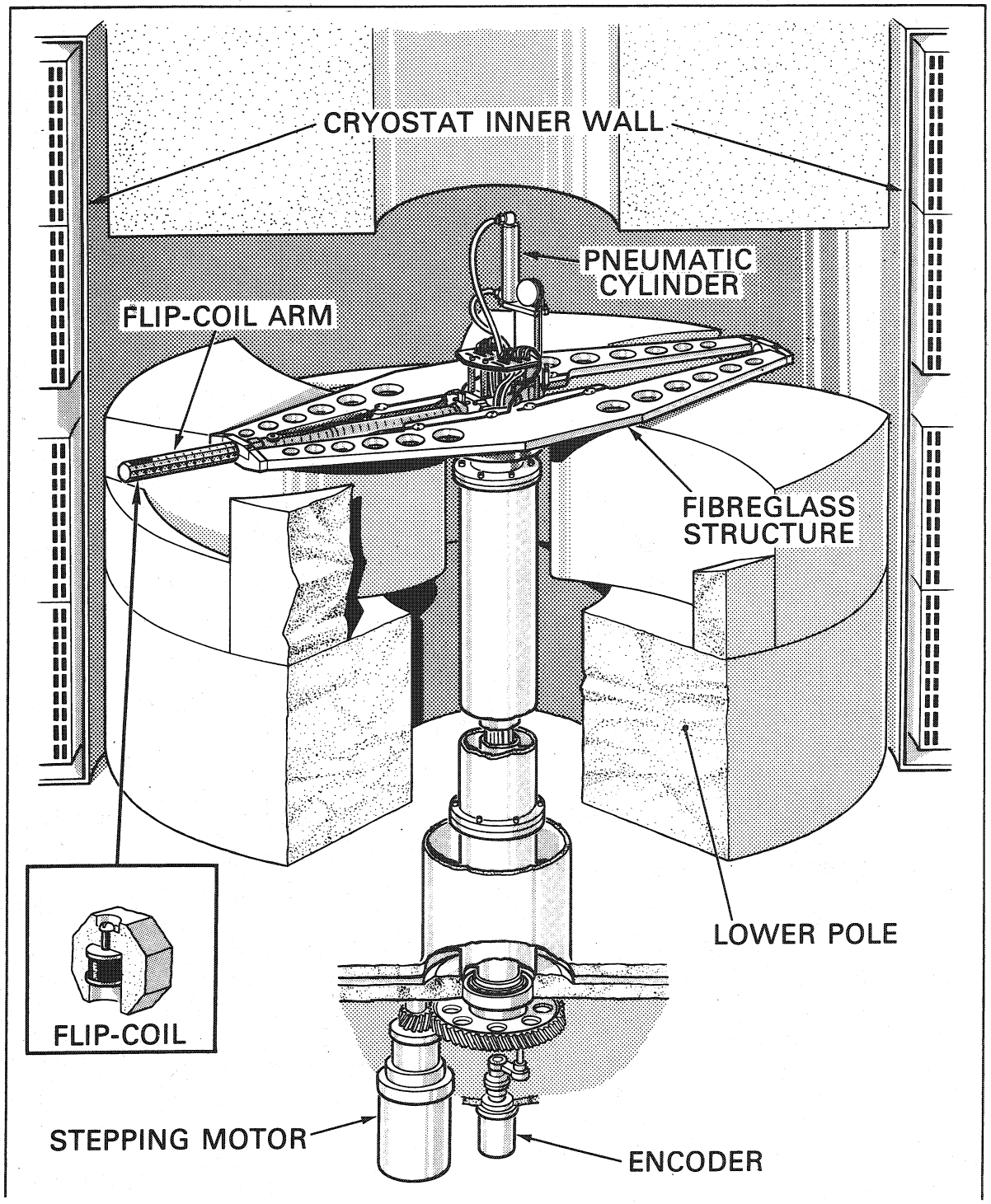

Fig. 3 Isometric view of field measuring apparatus.

the three outermost flip-coils is removable to permit measurements when the magnetic extraction elements are installed. The coils were flipped by rotating the arm 180° about its axis with a pulley driven by a pneumatic cylinder. The arm could be positioned around the azimuth of the cyclotron by a stepping motor mounted at the bottom of the lower pole. The azimuthal position was measured by an optical encoder with an accuracy of 0.044°.

Figure 4 shows an electrical schematic of the measuring system. The currents induced in the flip-coils were integrated by electronic integrators connected through a relay multiplexer to a 5-1/2 digit digital voltmeter. All actions such as positioning of the arm, flipping the coils, triggering the voltmeter, and discharging the integrators were initiated using CAMAC modules controlled by a PDP 11/34 computer. To reduce electromagnetic interference, all connections between the flip-coils and integrators were shielded, twisted pairs.

The flip-coil bobbins were made of MACOR*, a machinable glass-ceramic, chosen because of its high resistivity and low thermal expansion coefficient. The bobbins were 6.12 mm high with a diameter of 4.17 mm; the outer diameter of the coils was 8.7 mm. The height-to-radius ratio was chosen to minimize the second order error due to the finite sizes of the flip-coils[4]. Each layer-wound coil had approximately 1144 turns of AWG38 copper wire and a resistance of 53 ohms. The magnetic centre of each coil was determined in a magnetic field gradient and found to be within 0.02 mm of the geometric centre, therefore no special orientation of the flip coils on the arm was necessary.

---

* Corning Glass Works, Corning, New York.

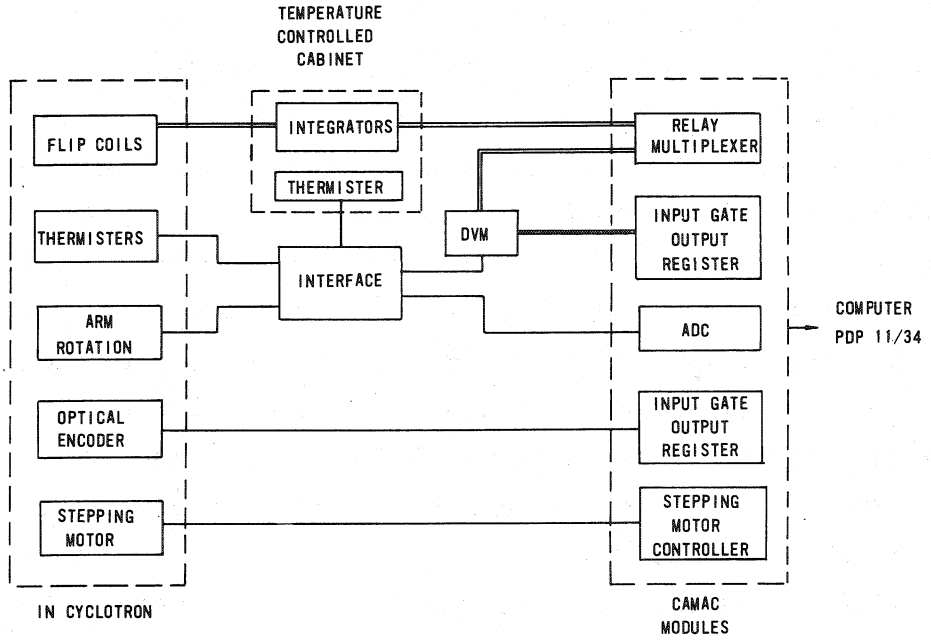

Fig. 4 Schematic of electrical connections of the field measuring apparatus.

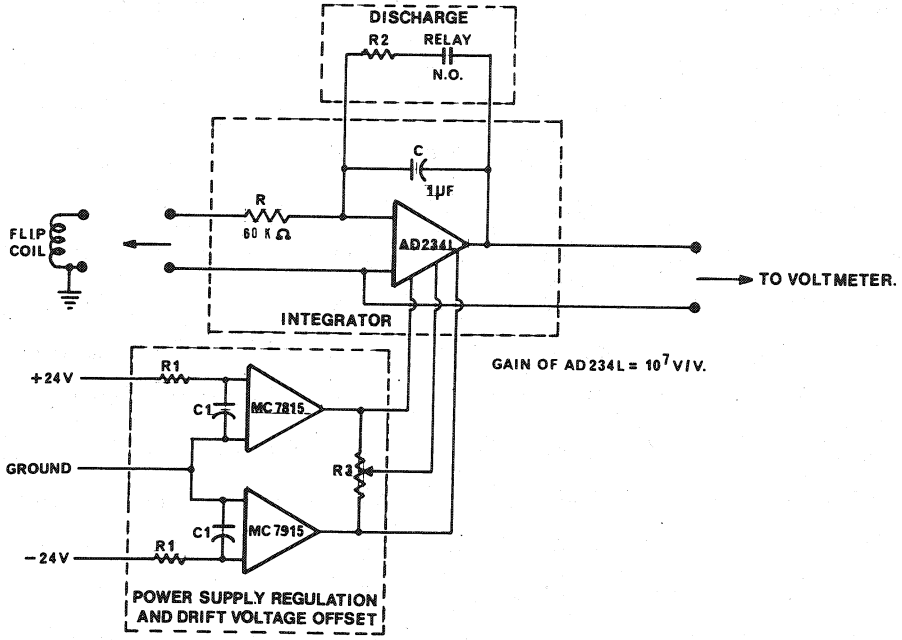

Fig. 5 Schematic of integrator.

Figure 5 is a schematic diagram of the integrator circuit which is similar to that used to measure the magnetic field in the Oak Ridge cyclotron[5]. A low noise, wide band chopper stabilized operational amplifier (Analog Devices AD234L) was chosen because of its low initial and thermal offset. The integrator resistance and capacitance were 60 kΩ and 1 μF respectively with the thermal coefficient of the RC values being -50 ± 50 ppm/°C. In order to reduce the thermal effect, the cabinet which housed these integrators was maintained at a temperature around 40°C and constant within 0.5°C. The RC product was chosen to give a calibration coefficient of ∿ 1.3 V/T so that in the maximum fields of ∿ 6 T, the integrator output would be less than 10 V.

Calibration

Each flip-coil with its integrator was calibrated with the apparatus shown in Fig. 6. The small electromagnet, mounted on ways, could be centered over any of the 40 flip-coils or an NMR probe located just beyond the end of the flip-coil arm. Calibration inductions from 0.2 to 1.0 tesla were used; at 1 T, the reduced homogeneity of the field limited the accuracy of the NMR reading to 1×10^{-4} which was taken as the accuracy of the calibration. The calibration procedure was as follows: The magnet was positioned over the NMR probe and the magnetic field measured. The magnet was then positioned over the flip-coil to be calibrated. Under computer control, the calibration coefficient was measured three times, the final value stored being the average of the measurements. The magnet was then repositioned over the NMR probe to check for magnet drift. If the field change was greater than 1×10^{-4}, the run was not used. The calibration procedure followed the same timing cycle as used for the actual field measurements (see below).

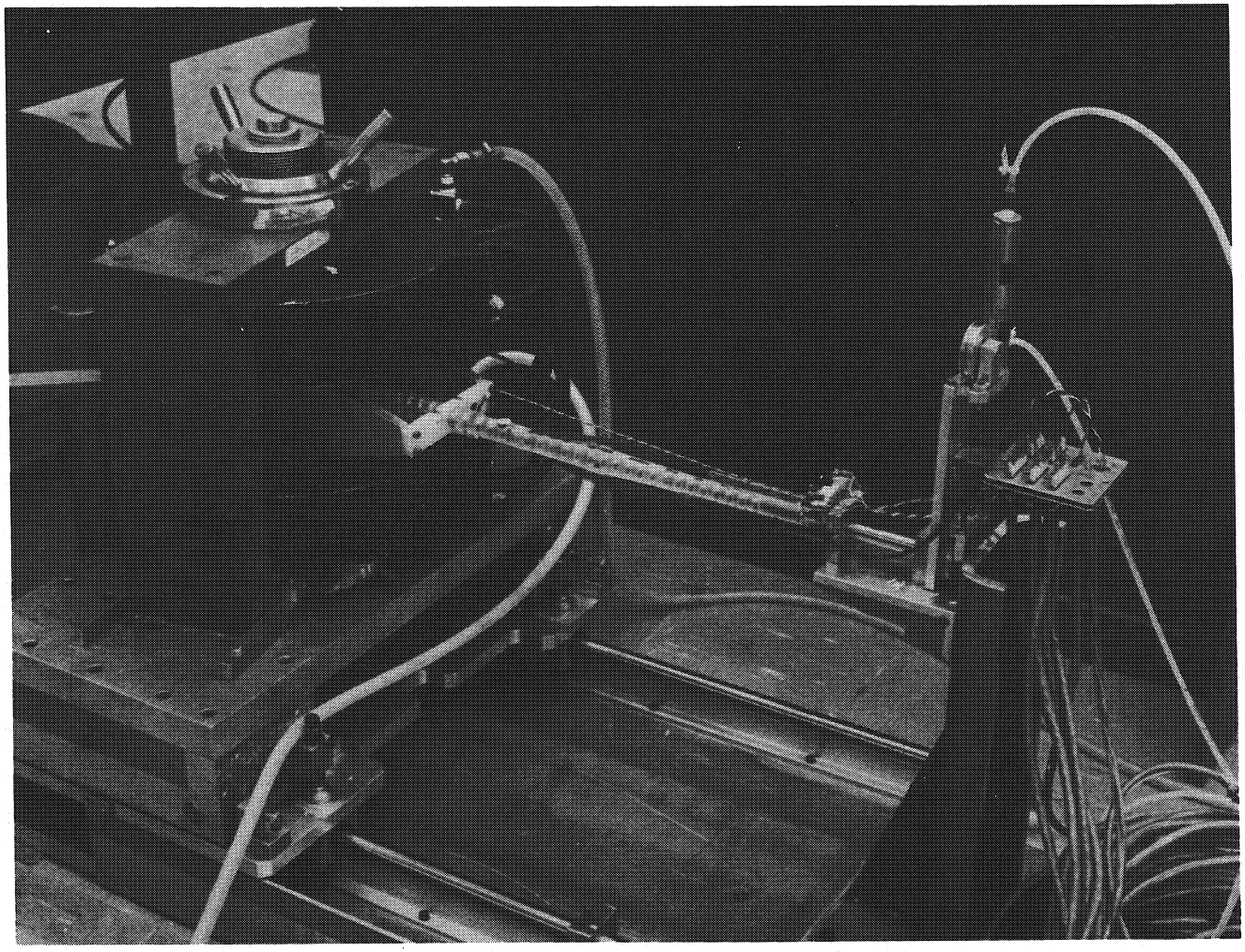

Fig. 6 Apparatus used to calibrate the flip-coils. The electromagnet at the left of the photograph is mounted on ways and can be positioned over any of the 40 flip-coils or an NMR probe just beyond the end of the flip-coil arm (the position shown in the photograph). The pneumatic cylinder and pulley arrangement used to flip the coils is seen at the right.

Typically four such measurements were made for each of the flip-coils. On one flip-coil (# 20), fifteen calibration runs were made over an interval of eight days. All save one of these runs were within 1×10^{-4} of the average, the exception being the calibration at the lowest induction, 0.2 T, which was 1.07×10^{-4} lower than the average. No field dependence was apparent in these calibrations.

One year later the flip-coils were again calibrated. The average of the 40 calibration coefficients had changed 6×10^{-5} and 29 of the calibration coefficients were within $\sqrt{2} \times 10^{-4}$ of their original values. For the other eleven, the greatest change in calibration coefficient was $+6.1 \times 10^{-4}$ and the second greatest change -4.2×10^{-4}. After a further six months, the outer 28 flip-coils were intercalibrated in a large dipole at an induction of 1.6 T. Four of the coefficients differed by more than expected and these four flip-coils were within the subset of eleven anomalous flip-coils noted above.

We interpret the larger than expected differences in the remeasured calibration coefficients of the eleven flip-coils as changes in the integrating capacitors. "Good" and "bad" capacitors are a hazard in this type of apparatus and such behaviour is not unexpected[6]. The average change of 6×10^{-5} could be due to several causes - a temperature change in the integrator temperature controlled cabinet (the regulator was replaced), a change in the digital voltmeter calibration or a general change in the capacitors.

We conclude that the accuracy of our calibration to $\pm 1 \times 10^{-4}$ is valid for only a finite period - at least for eleven of our forty flip-coils, and recalibration will be necessary before any further mapping. However, the precision

of our measurements from individual flip-coils is much better than 1×10^{-4} and it is this superior precision that permits the accurate measurement of the first and second Fourier components of the fields.

The precision of the field measurements is shown in Fig. 7 where the distributions of the differences from the average of 100 successive measurements taken at three different inductions are plotted for a given flip-coil. The 1.6 T results were taken in the first dipole of the Chalk River Q3D spectrometer, the other two in the cyclotron. Superposed on each histogram is the normal curve of error for the calculated probable error of the distribution which is almost independent of induction. The two lower curves also include a component from field fluctuations which are obviously small compared to the main cause of error - variations in integrator drift. For measurements in the cyclotron ($B > 2$ T) our"short-term" precision for individual flip-coils is better than 1×10^{-5}, allowing measurements of the first and second harmonic fields with this apparatus.

The calibration coefficient of a flip-coil is directly proportional to its area and therefore depends on the ambient temperature. The coefficient of thermal expansion of the MACOR bobbins is approximately half that of copper, and for temperatures greater than the temperature at which the coils were wound it is the thermal expansion coefficient of copper that will determine the change in the calibration coefficient. A crude check of the temperature coefficient of flip-coil # 20 was made by warming the entire flip-coil arm by 8^{o}. The measured coefficient was $3.9 \times 10^{-5}/^{o}C$, 20% greater than the calculated value of $3.3 \times 10^{-5}/^{o}C$, but within the experimental error of the measurement. The

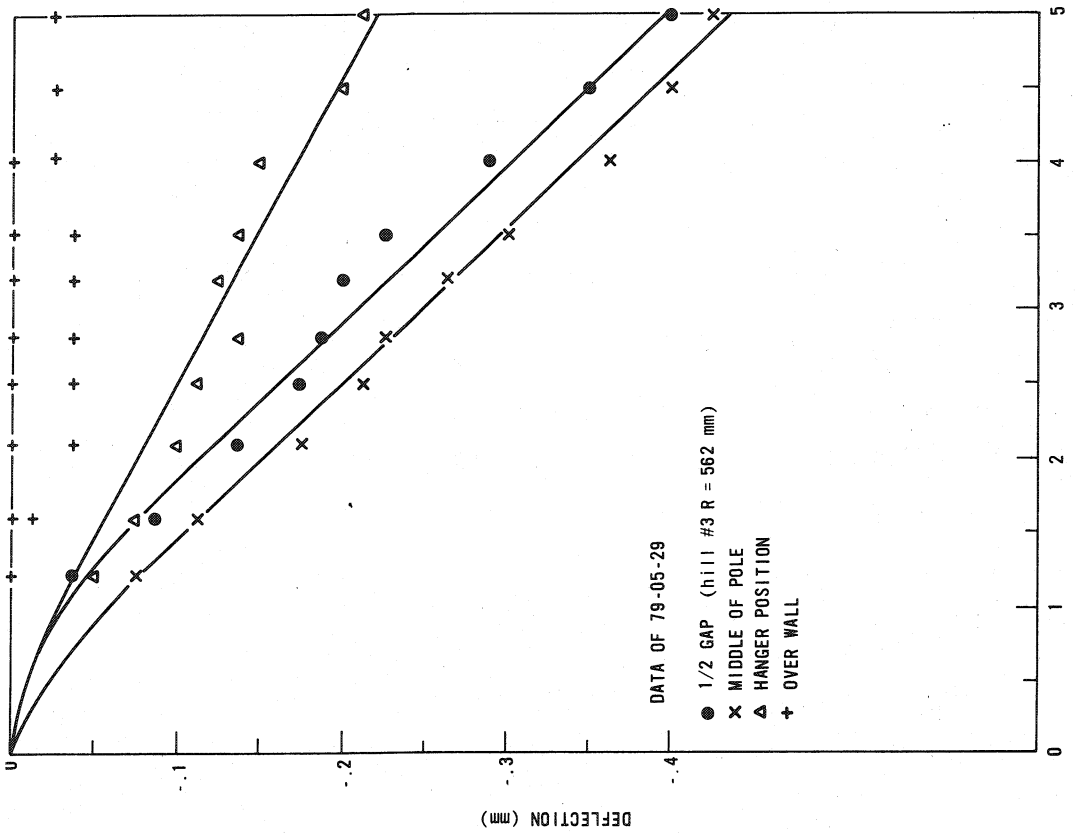

Fig. 8 Deflections of upper pole from magnetic forces.

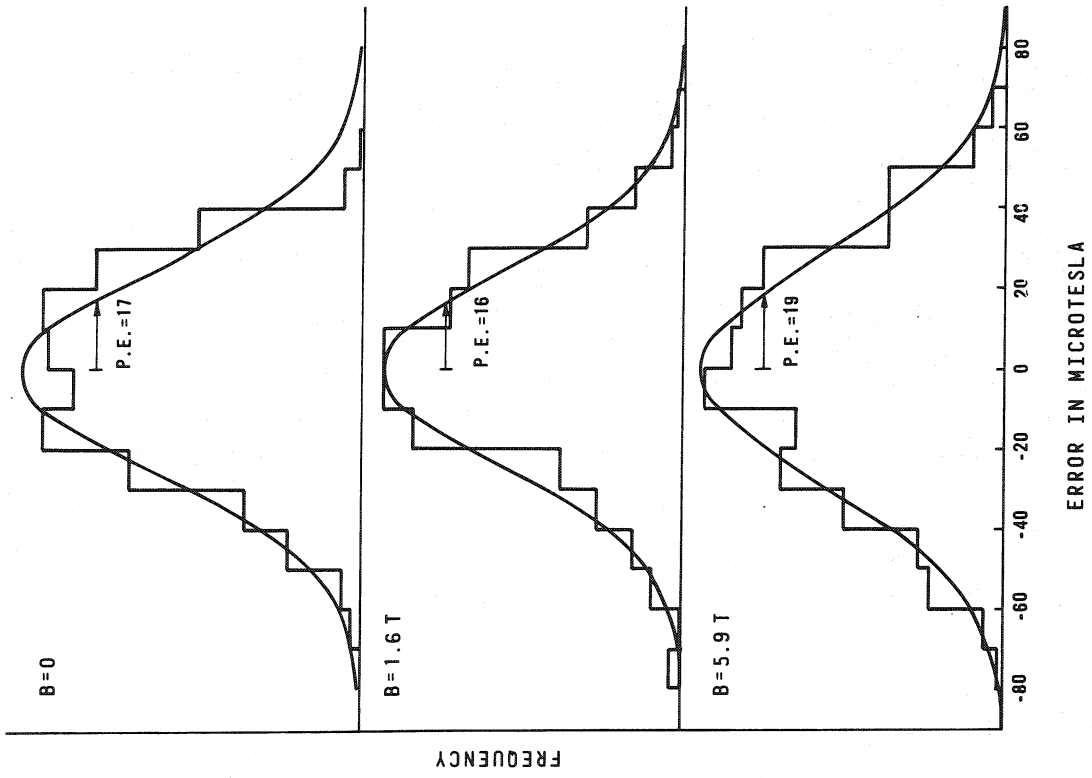

Fig. 7 Distributions of induction differences from the average of 100 successive measurements taken at three different inductions.

measurements reported here were taken with the arm temperature 21.5 ± 1.8°C. This translates into a $\pm 6 \times 10^{-5}$ variation in the calibration coefficient (within the accuracy of our calibration) and no corrections were made for this effect. It should be noted that in terms of the short-term precision of our measurements, the flip-coils were enclosed by the 150 tonne magnet and temperature changes of the flip-coils occurred with the magnet's thermal time constant (many hours). The arm temperature was monitored throughout the measurements and a change greater than 0.1°C between the beginning and end of a typical 50 minute run was unusual.

Measurement Technique

The apparatus was controlled and the data collected by a PDP 11/34 computer (operating under MUMTI - Multi User Multi Task Interpreter)[7] using one crate of the serial CAMAC highway.

The magnetic field at a given azimuth was measured using the following sequence:

1. short circuit integrator inputs and wait 3 seconds
2. scan integrator outputs (∿ 6 seconds)
3. rotate arm 180°, i.e. flip coils (∿ 3 seconds)
4. scan integrator outputs (∿ 6 seconds)
5. rotate arm back 180°, i.e. flop coils (∿ 3 seconds)
6. scan integrator outputs (∿ 6 seconds)
7. advance arm 2° in azimuth (∿ 3 seconds)
8. scan integrator outputs (∿ 6 seconds).

The readings were corrected for integrator drift by subtracting the average of the readings taken at steps 2 and 6 from those at step 4. This procedure required approximately

100 minutes to complete a 360° map. A faster procedure requiring only 49 minutes for a complete map is to flip the arm at 10° intervals and repeat only steps 7 and 8 at the intervening 4 angles then calculate the intermediate points from the field differences. The latter method was used for most of the results reported here.

The method of correcting the measurements for integrator drift assumes a constant drift rate and errors are introduced by fluctuations in the drift rate. These fluctuations are one of the principal causes of the spread in the results shown in Fig. 7. This was demonstrated by initiating a series of scans of the integrators at 9 s intervals and recording the difference between each reading and the average of its adjacent readings. The flip-coils were in a field free region and the arm was not flipped throughout these measurements. The distribution of these differences was $\sim$ 60% of the width of the upper histogram in Fig. 7.

The stepping motor that rotates the flip-coil arm requires approximately 10 pulses to advance the optical encoder one bit. This feature was used to reposition the flip-coil arm with approximately an order of magnitude better reproducibility than the accuracy of the encoder by the following procedure: The arm was advanced until the optical encoder was one bit less than that required. The stepping motor was then advanced one step at a time, reading the encoder between each step until the encoder readout was at the desired value. This improved reproducibility is important, especially when comparing Fourier components of field maps when centering the coil. The precision of repositioning the arm was measured near a hill edge where the azimuthal gradient is $\sim$ 0.2 T/degree.

Successive measurements in this gradient were made after 360° rotations of the arm and agreed to better than 0.2 mT.

The procedure of shorting the integrators after flipping the coils back and forth ensured a relatively small voltage on the capacitors when they were discharged. This minimized the error introduced by the voltage transient that appeared across the integrator output after a rapid voltage change across the capacitors. The amplitude of this transient is a function of the time rate of change of the input voltage, $\sim$ 1 mV per V/s, and decays with a time constant of 1/3 seconds.

A similar voltage transient appears, of course, after the coils are flipped. The nature of the voltage variation with time from a flipped coil (approximately sinusoidal) and a 300 ms delay built into the program after the arm is flipped reduces the calculated amplitude of this transient. If V_i is the final integrator voltage, then when the first flip-coil is read, the transient is $6 \times 10^{-5} V_1$, and has decayed to less than $1 \times 10^{-5} V_6$ when the sixth flip-coil is read; it is less for succeeding flip-coils. This effect was noted after the measurements reported here were taken; future measurements will include an additional half second delay between flipping the arm and scanning the integrators so that for all integrators, the transient is less than $1 \times 10^{-5} V_i$.

Centering of the Superconducting Coil and Positional Stability

The superconducting coil was centered on the axis of the field measuring apparatus which had been centered on the axis of the poles using the first Fourier component of the magnetic field measured with the three outermost flip-coils.

The first harmonic component in any map is the sum of contributions from:

1) residual first harmonic from manufacturing tolerances.
2) displacement of the axis of the field measuring apparatus from the field center.
3) lateral displacement of the upper pole from the lower pole.
4) displacement of the superconducting coils from the axis of the poles.
5) accuracy of the optical encoder used to position the azimuth of the arm holding the flip-coils (difficult to separate from 1)).
6) precision of the measured field at each point (better than 0.1 mT).
7) effects of external elements (e.g. injection and extraction dipoles, asymmetries in the yoke).

Fortunately, many of these are separable because the different contributions have characteristics that differ with average induction and radius.

The upper pole was initially positioned by passing two trim rods through the upper pole and into the corresponding trim rod holes in the lower pole. This procedure aligns the two poles within 0.3 mm. The axis of the field measuring apparatus was then adjusted to minimize the first harmonic measured by the three outermost flip-coils at an average induction of 1.2 T (inner-coil current = outer-coil current = 100 A). The three outer flip-coils were chosen because they measure the field where the radial gradient is greatest at this excitation: 2.4 T/m for flip-coil # 38, 7.4 T/m for # 39 and 14.3 T/m for # 40. The magnet excitation of 100 A/100 A was chosen because it is low enough to introduce only a small

effect from coil decentering while saturating the hills, thereby reducing effects from variations in permeability. Once these adjustments were completed the axis of the field measuring apparatus was defined as the center of the cyclotron.

The superconducting coil was then centered using the first harmonic measured at the same three flip-coils at an average induction of 3.2 T. At this excitation, the contribution to the induction from the coil currents is $\sim$ 2 T and we assume superposition of the iron and current components. The gradient due to the coil currents is 1.0, 1.6 and 2.0 T/m for the radii of flip-coils 38, 39 and 40, respectively.

Any movement of the poles or coil causes little change in the first harmonic at interior radii where $d\langle B\rangle/dR$ is small; the reproducibility of the first harmonic measurements in this region was ±0.035 mT or better. This means we can detect displacements of the "poles" from the axis of the field measuring apparatus of 0.0025 mm and displacement of the coil of 0.018 mm. The sensitivity to coil displacements is approximately three times the required placement accuracy of 0.05 mm[8].

The axis of the coil was initially placed 1.4 mm off the machine axis. The first adjustment reduced this displacement to 0.3 mm and two subsequent adjustments further reduced this to 0.1 mm. Better positioning was not attempted, but the sensitivity of the first harmonic to radial displacements of the coil clearly permits more accurate centering.

"Centering runs", consisting of a complete map at 1.2 T immediately followed by a map at 3.2 T, were taken

periodically over a two month interval. Throughout this period, relative to the axis of the field measuring apparatus, the axis of the coil remained at its original displacement of 0.1 mm within ±0.01 mm; we conclude that, within the ±0.018 mm uncertainty in the measurements, the coil did not move radially.

The lower pole (on which the field measuring apparatus is mounted) is lowered by jackscrews for normal access to the midplane and is reseated within 0.02 mm by linear bearings. The upper pole is bolted to the upper end ring and is not scheduled to be dowelled to it until the cyclotron is reassembled at its final location in the nuclear physics laboratory. During the measurements reported here the upper pole moved south by 0.06 mm. This displacement was detected by the first harmonic measurement made at 1.2 T and confirmed by the upper pole positioning micrometers. The cause of this displacement is attributed to repeated "dishing" of the pole under excitation. At $\langle B \rangle$ = 5 T, the attractive force between the poles is 10 MN. Figure 8 shows, as a function of midplane induction, the deflections of the upper pole top surface and the closing of the midplane gap[9]. It is this flexing that caused the movement of the upper pole, but such radial motion should not occur after the pole is dowelled to the upper end ring.

The superconducting coil is suspended from the upper end ring by 12 hangers. As the magnet is excited, the entire coil moves up and down with the flexing of the end ring. As shown in Fig. 8, the range of this motion over the operating inductions from 2.5 to 5 T is 0.1 mm, one-half of the required alignment of the coil and magnet midplanes[8]. We conclude that the radial and axial stability of the coil position is adequate.

Mapped Fields

Figure 9 shows the inner and outer coil currents at the 48 field mapping points. Also shown are equi-induction contours for R = 407 mm. As a representative sample of the reduced results Tables I, II and III list the average inductions as well as the amplitudes and phases of the first and second harmonic components at the 40 flip-coil radii.

Figure 10 illustrates how the radial gradient of the magnetic field varies as a function of the difference current and the average magnetic induction.

Figure 11 shows how well the calculated fields agree with the measurements. The comparison of the calculations with the measurements is discussed in more detail elsewhere[3].

Field Stability and Reproducibility

The stability of the magnetic field was measured with the field measuring apparatus fixed at one azimuth and measurements taken at 20 second intervals over a period of 45 minutes. As stated above, the principal contribution to the width of the distribution in Fig. 7 is the variation in the integrator drifts. These are random fluctuations, and for the stability measurements, the 40 flip-coil voltages were summed to give a better than six-fold reduction in the variations from instrumental effects. Figure 12 shows the magnetic field variations thus measured at a midplane induction of 5 T. The extreme variation was 11 ppm. The measurement was repeated with the magnet power supply turned off to measure the instrumental contribution. The peak to peak excursions of the summed voltages corresponded to 3.5 ppm (compared to 11 ppm above), in excellent agreement

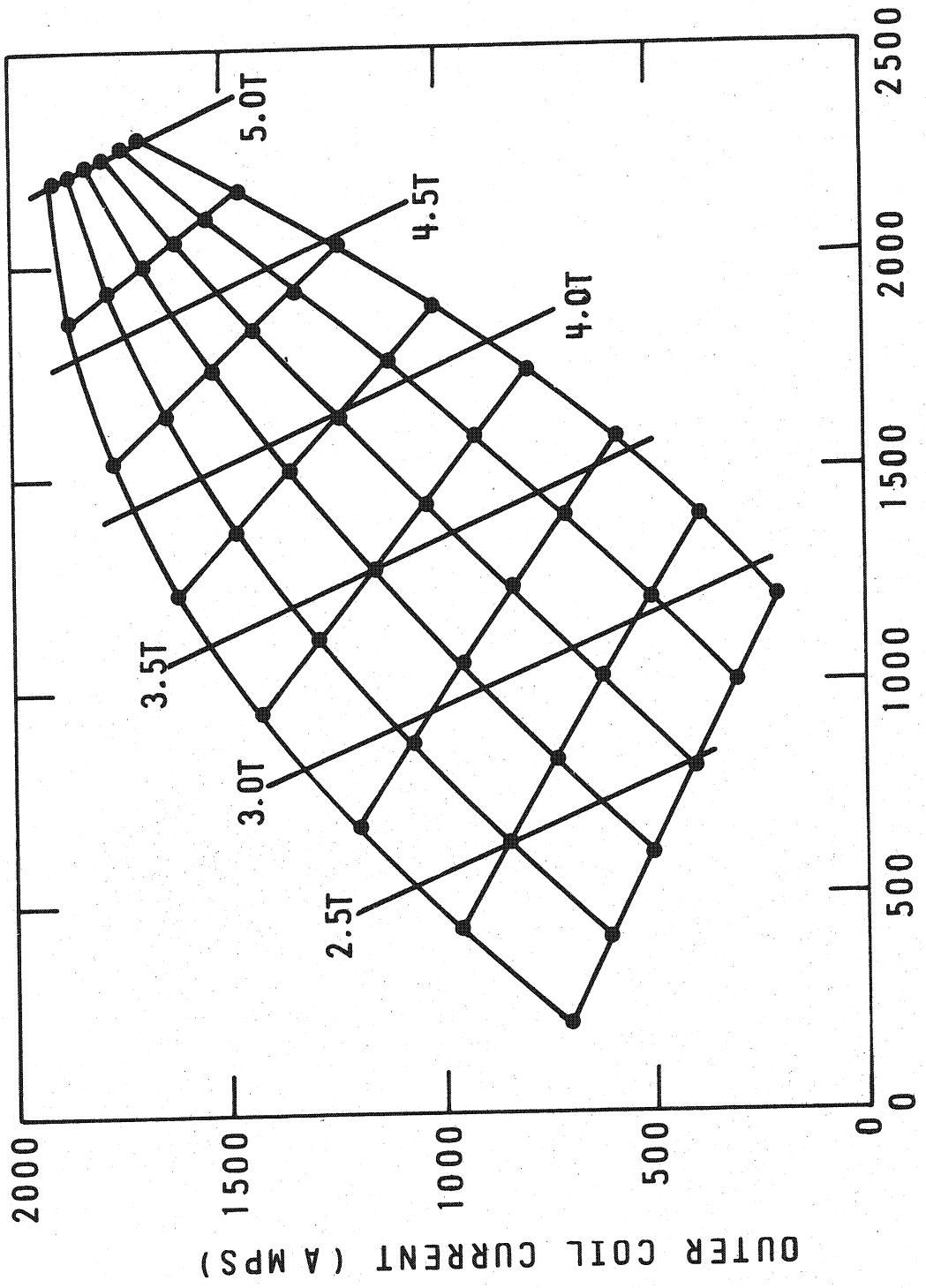

Fig. 9 Inner- and outer-coil currents for the 48 field mapping excitations. Also shown are lines of equal induction from 2.5 to 5 tesla.

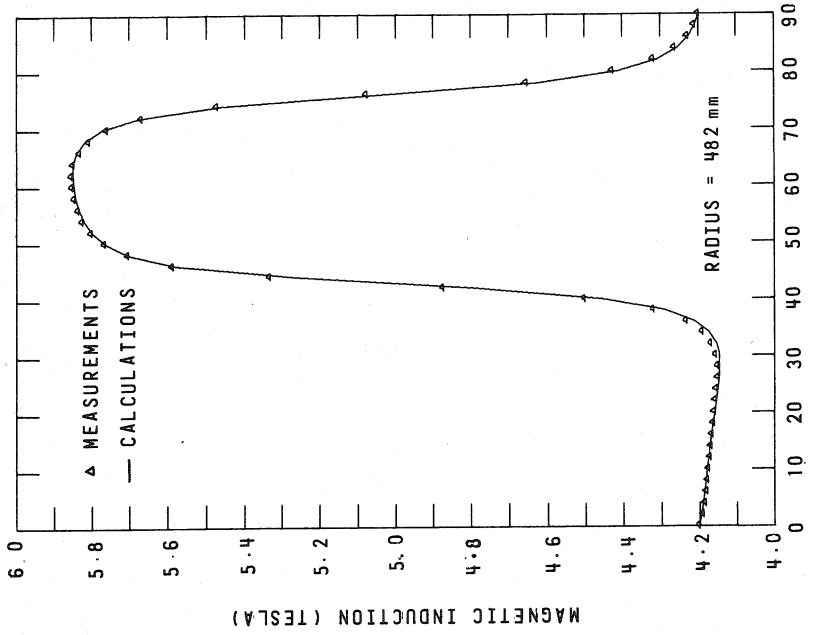

Fig. 11 Comparison of measured and calculated inductions over one quadrant at R = 482 mm.

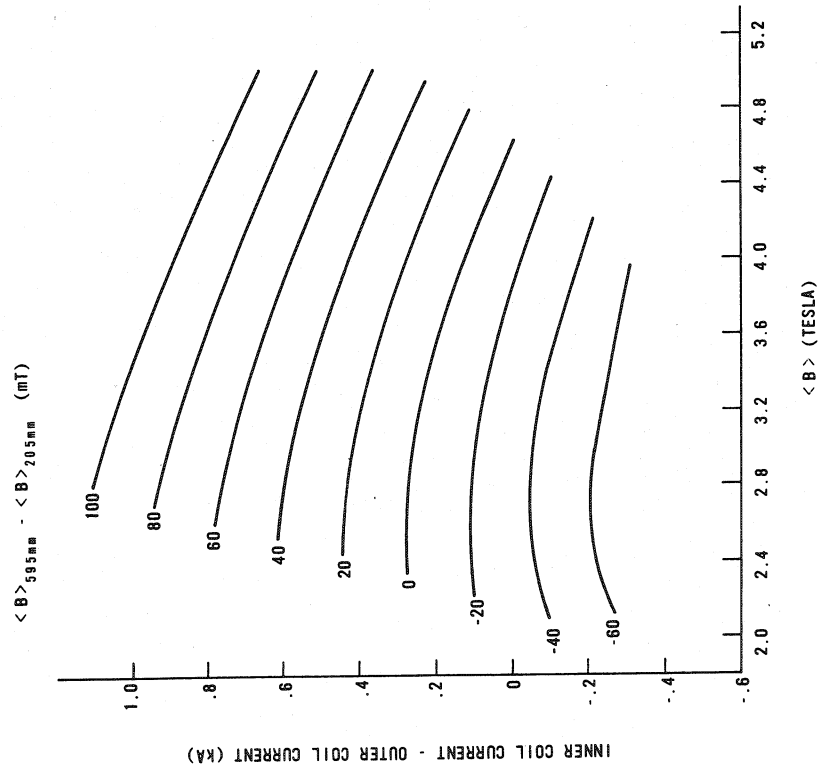

Fig. 10 Variation of the radial gradient as a function of the difference current and average midplane induction.

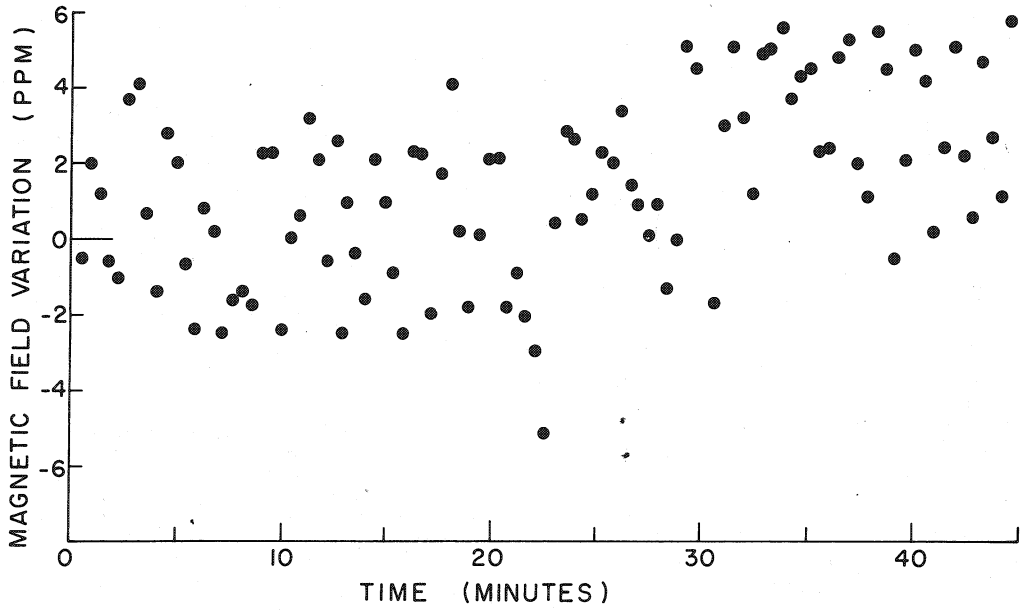

Fig. 12 Variation with time of the midplane field at full excitation.

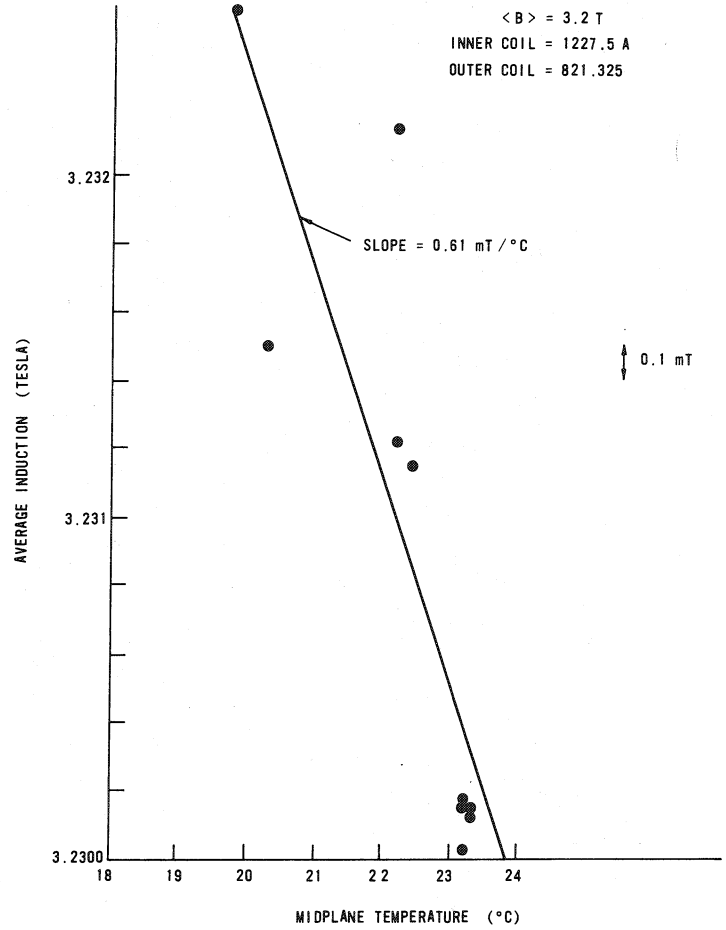

Fig. 13 Variation of the midplane induction as a function of the midplane air temperature.

with the uppermost histogram in Fig. 7 which is for a single flip-coil.

Short-term (< 20 second) fluctuations of the magnetic field were measured by the voltage induced in a 20-turn coil wound around the skirt on the lower pole (see Fig. 1). These fluctuations were even less than the measurements reported above.

Variations in the average magnetic field will change the beam output energy. For the worst case (product of turns and radiofrequency harmonic number = 400), the energy spread so introduced is an order of magnitude less than the inherent spread in a 3^{o} bucket.

The 3.2 T field map from each centering run was also used to measure the run-to-run reproducibility of the magnetic field. The principal cause of the measured variations in the midplane induction was due to the temperature coefficient of the saturation magnetization of steel. This was not deduced until near the end of the measurements and outside yoke temperatures were not recorded. The yoke was housed in a building that was not air-conditioned and the temperature outside the building varied from 2^{o} to 32^{o}C over the period of the reproducibility measurements. Figure 13 shows the average induction measured with flip-coils 20 through 25 as a function of the midplane air temperature. The thermal time constant of the yoke is several hours and the midplane air temperature was but an approximation to the average steel temperature. This uncertainty in the yoke temperature probably contributes to the scatter of the results from the least squares linear fit (0.61 mT/^{o}C) and to the difference from the published value[10] of 0.37 mT/^{o}C. A systematic investigation of this effect will be made when the field is remapped.

The five measurements at the bottom of the figure were taken when the temperature was relatively constant and show a resettability within 0.2 mT.

First and Second Harmonic Amplitude

Once the coil is centered, first and second harmonic amplitudes still exist from manufacturing and assembly tolerances, asymmetries in the yoke midplane penetrations, magnetic extraction channel components and the injection and extraction dipoles. Figure 14 shows how these last four sources depart from 4-fold symmetry. The philosophy has been to eliminate, or reduce, the first harmonic from any cause by an equivalent compensation and then reduce the residual to an acceptable level with the trim rods. The second harmonics that have been calculated (and in some cases measured) are small enough to be tolerated without compensation. Only the effects from manufacturing and assembly tolerances and asymmetric midplane penetrations of the yoke are reported here - the magnetic channel, injection and extraction dipoles were not installed for these measurements.

In Fig. 14, the two unlabeled holes in the yoke wall on the right-hand side of the figure compensate the first harmonic generated by the other midplane holes shown in the figure. The first harmonic could be compensated by a single, awkwardly shaped hole but by using two holes, fabrication was simplified. The size of the compensating holes was calculated at each yoke wall radius to generate an equal and opposite first harmonic to that created by the other midplane holes at that same radius thereby compensating at all radii.

Figure 15 shows the measured amplitude of the first harmonic component as a function of radius for an average

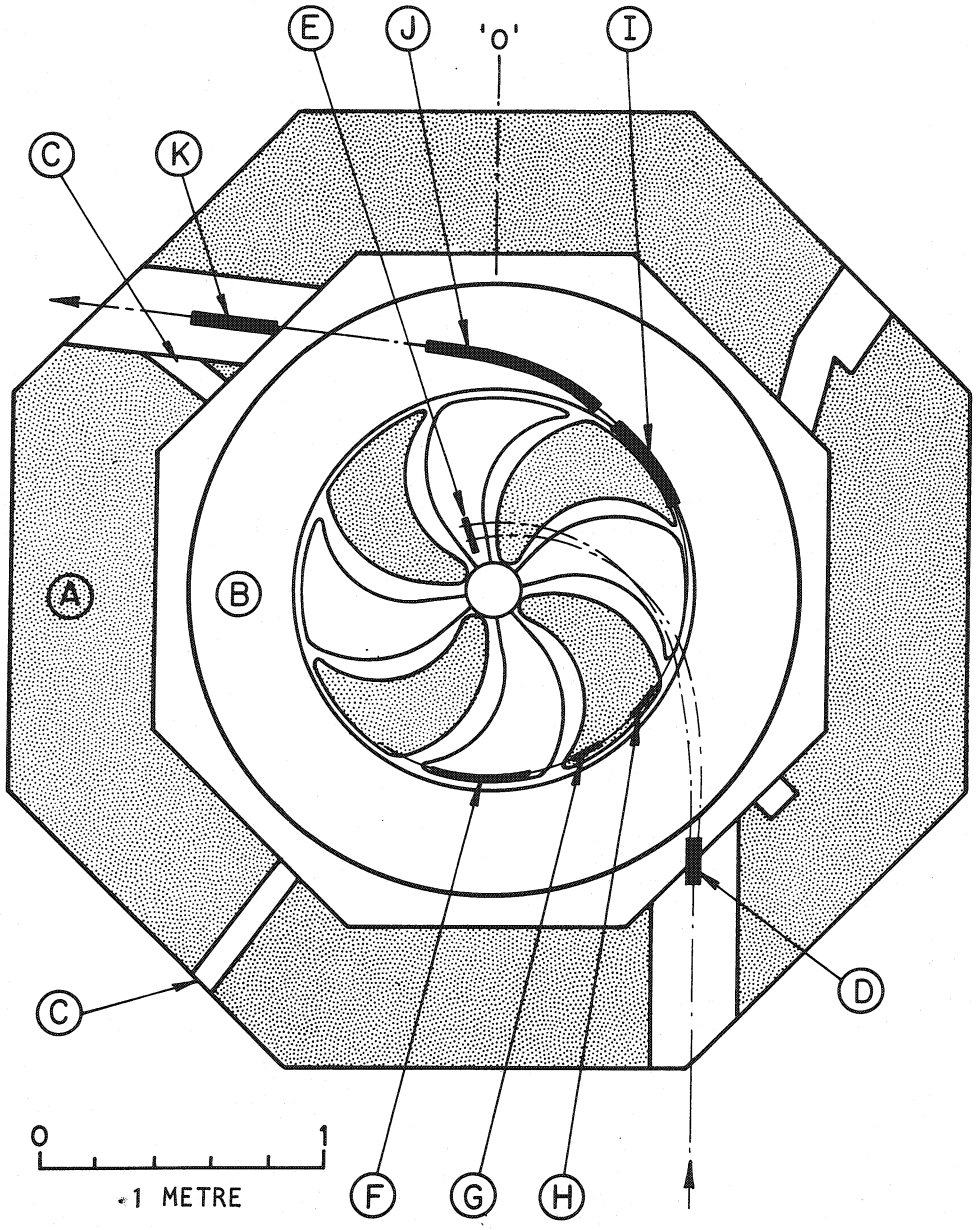

Fig. 14 Midplane plan view of the cyclotron: A - yoke, B - cryostat, C - probe hole, D - injection steering magnet, E - stripping foil, F - electrostatic deflector, G, H, I, J - magnetic extraction channel components, K - extraction steering magnet. The two unlabeled holes on the right are for first-harmonic compensation.

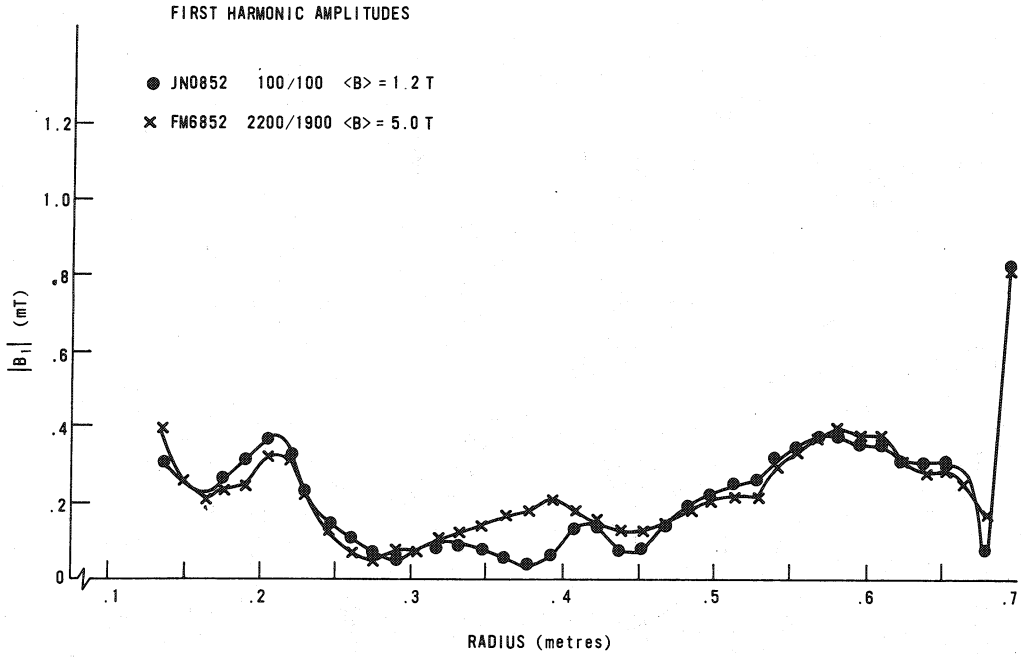

Fig. 15 First harmonic amplitudes as a function of radius for an average midplane induction of 1.2 and 5 tesla.

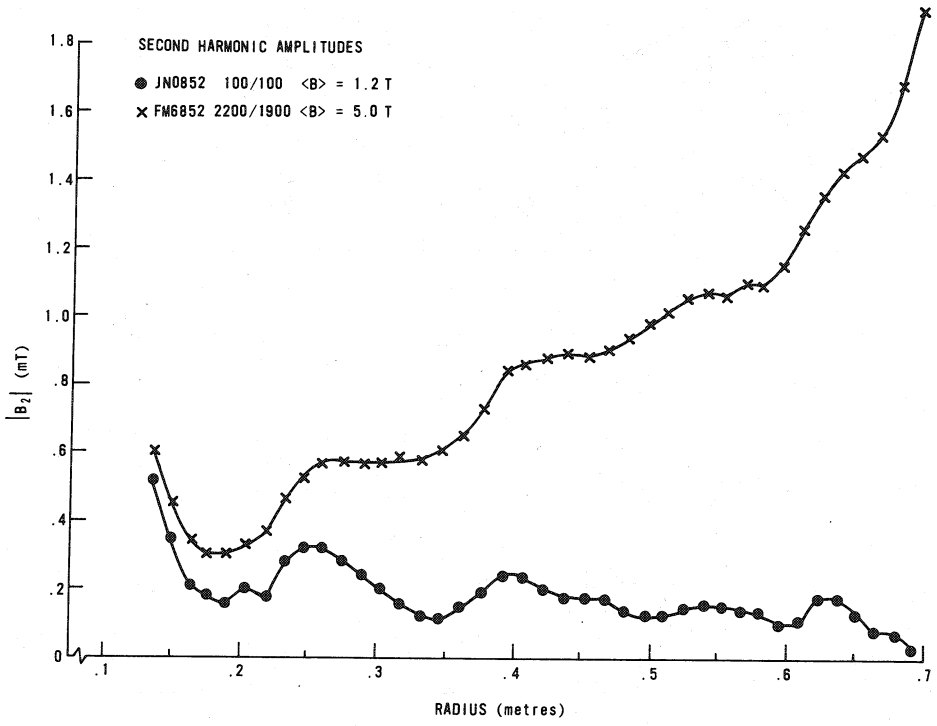

Fig. 16 Second harmonic amplitudes as a function of radius for an average midplane induction of 1.2 and 5 tesla.

midplane induction of 1.2 T and 5 T. At 1.2 T, the hills are saturated ($B_{Hill} \sim 2.2$ T) but the induction in the yoke walls is $\sim$ 0.5 T, hence the first harmonic at all radii is due almost entirely to flutter pole manufacturing and assembly tolerances.

The small change in the first harmonic at <B> = 5 T shows that the yoke wall compensating holes work well and that coil imperfections give a negligible contribution. For example, the calculated first harmonic from uncompensated yoke holes at r = 650 mm is 2.1 mT, more than an order of magnitude greater than the measured difference. The maximum amplitude in the acceleration region, 150 < r < 650 mm, is less than 0.4 mT, well within the capability of compensation by the trim rods. However, because the first harmonic is mainly due to imperfections in the flutter poles and almost independent of field level it can be significantly reduced by modest shimming of the flutter poles. This will be done after the next round of field mapping on the modified flutter poles.

Figure 16 shows the measured amplitude of the second harmonic component as a function of radius for the same excitations as Fig. 15. Again, the amplitude at <B> = 1.2 T is caused mainly by the flutter pole manufacturing and assembly tolerances. The amplitude at <B> = 5 T increases to 1.9 mT at R = 693 mm and is less than half the value calculated for the holes in the yoke walls. If the <B> = 1.2 T results and the calculated values for the midplane yoke holes are vectorially subtracted from the <B> = 5 T data, the resulting second harmonic has the characteristic shape of a coil imperfection. A second harmonic of approximately this magnitude is expected from the ellipticity

introduced by double pancake crossovers. The magnitude of the second harmonic over the whole operating range is well within acceptable limits and the azimuth is such that it will reduce the larger but still acceptable second harmonic from the extraction system.

Acknowledgements

It is a pleasure to acknowledge the assistance of W. McAlpin, R.E. Milks and K.B. Tait in the design of the apparatus, R.L. Graham, L.G. Hansen and R.B. Walker in the computer control, C.B. Bigham, L.F. Birney, K.A. Dobbs, E.A. Heighway, C.R. Hoffmann, A.B. Hood, J.A. Hulbert, H.R. Schneider and Q.A. Walker in magnet operation.

Table I

Reduced Data of a Mapped Field

FILENAME=FM5151.JH0
INNERCOILCURRENT= 0.4000000E+03
OUTERCOILCURRENT= 0.6000000E+03

	FIRST AND SECOND HARMONIC FIELDS					
X	R	B0	B1	PHI1	B2	PHI2
	MM	TESLA	MT	DEG	MT	DEG
1	135	2.0737	.3936	74	.5767	86
2	149	2.1033	.2483	41	.4004	82
3	163	2.1084	.1577	2	.2621	82
4	177	2.1051	.1717	-24	.2304	85
5	191	2.0963	.2249	-16	.2055	97
6	205	2.0909	.2979	-5	.2349	111
7	219	2.0888	.3045	-3	.2539	97
8	233	2.0867	.1954	0	.3468	83
9	247	2.0847	.1164	11	.3845	86
10	261	2.0806	.6799E-01	49	.3991	94
11	275	2.0760	.4397E-01	108	.3815	98
12	289	2.0721	.4073E-01	88	.3422	100
13	303	2.0692	.3369E-01	34	.3144	101
14	317	2.0662	.4806E-01	14	.3023	103
15	332	2.0634	.4713E-01	16	.2718	101
16	347	2.0607	.4685E-01	3	.2538	97
17	362	2.0572	.3112E-01	-60	.2849	91
18	377	2.0544	.3715E-01	187	.3640	92
19	392	2.0509	.8984E-01	202	.4334	91
20	407	2.0490	.1139	222	.4325	93
21	422	2.0477	.9811E-01	223	.3992	96
22	437	2.0463	.8835E-01	206	.3568	99
23	452	2.0451	.1374	162	.3232	99
24	467	2.0444	.1921	161	.3106	97
25	482	2.0429	.2118	164	.2932	99
26	497	2.0413	.2485	159	.2990	100
27	511	2.0400	.2712	155	.3034	98
28	525	2.0386	.2787	152	.3185	99
29	539	2.0382	.3397	151	.3172	98
30	553	2.0381	.3794	151	.2852	98
31	567	2.0382	.4249	150	.2567	101
32	581	2.0393	.4468	157	.2372	103
33	595	2.0404	.4289	164	.2099	109
34	609	2.0429	.4246	171	.2813	115
35	623	2.0445	.3857	182	.3563	118
36	637	2.0426	.3477	195	.3518	119
37	651	2.0313	.3660	193	.3000	123
38	665	1.9978	.3200	188	.2483	124
39	679	1.9106	.2281	265	.2532	130
40	693	1.7273	.9307	-58	.2716	-36

Table II

Reduced Data of a Mapped Field

FILENAME=FM1351.JHO
INNERCOILCURRENT= 0.1578200E+04
OUTERCOILCURRENT= 0.5740000E+03

	FIRST AND SECOND HARMONIC FIELDS					
X	R	B0	B1	PHI1	B2	PHI2
	MM	TESLA	MT	DEG	MT	DEG
1	135	3.4117	.4367	72	.5723	85
2	149	3.4483	.2499	32	.4333	81
3	163	3.4583	.1843	0	.3184	81
4	177	3.4599	.2091	-23	.3027	83
5	191	3.4544	.2516	-19	.2709	93
6	205	3.4528	.3240	-10	.2843	105
7	219	3.4547	.3030	-10	.3231	95
8	233	3.4564	.2151	-15	.4284	86
9	247	3.4588	.1138	-14	.4802	87
10	261	3.4591	.4259E-01	-25	.4876	94
11	275	3.4588	.3638E-01	254	.4885	97
12	289	3.4599	.6063E-01	261	.4666	99
13	303	3.4623	.7647E-01	-71	.4477	100
14	317	3.4645	.9203E-01	-56	.4472	101
15	332	3.4673	.9367E-01	-62	.4307	100
16	347	3.4706	.1020	-76	.4450	99
17	362	3.4727	.1260	-86	.4920	96
18	377	3.4764	.1351	248	.5574	95
19	392	3.4793	.1725	238	.6399	94
20	407	3.4837	.1798	237	.6389	95
21	422	3.4888	.1840	255	.6200	98
22	437	3.4938	.1407	258	.5726	101
23	452	3.4995	.1461	229	.5350	101
24	467	3.5063	.1546	216	.5268	102
25	482	3.5119	.2063	212	.5092	103
26	497	3.5172	.2251	205	.5082	104
27	511	3.5225	.2386	203	.4895	105
28	525	3.5274	.2333	194	.4834	106
29	539	3.5338	.2854	178	.4688	104
30	553	3.5400	.3288	171	.4297	104
31	567	3.5454	.3645	170	.3735	106
32	581	3.5511	.3871	173	.3436	109
33	595	3.5548	.3925	181	.3027	116
34	609	3.5595	.4018	187	.3511	123
35	623	3.5610	.3855	197	.4103	127
36	637	3.5563	.3684	206	.4102	134
37	651	3.5389	.3716	206	.4229	-37
38	665	3.4942	.3438	206	.4841	-27
39	679	3.3852	.3309	267	.6316	-20
40	693	3.1707	.9247	-60	.9372	-14

Table III

Reduced Data of a Mapped Field

FILENAME=FM1851.JH0
INNERCOILCURRENT= 0.2300000E+04
OUTERCOILCURRENT= 0.1690000E+04

	FIRST AND SECOND HARMONIC FIELDS					
X	R	B0	B1	PHI1	B2	PHI2
	MM	TESLA	MT	DEG	MT	DEG
1	135	4.9134	.4027	67	.5592	86
2	149	4.9533	.2245	29	.4513	83
3	163	4.9646	.1827	-7	.3274	84
4	177	4.9683	.2134	-32	.3008	87
5	191	4.9641	.2195	-24	.2980	98
6	205	4.9637	.3019	-15	.3333	108
7	219	4.9670	.3055	-17	.3517	99
8	233	4.9699	.2226	-25	.4555	89
9	247	4.9734	.1225	-35	.5092	92
10	261	4.9751	.7502E-01	-62	.5611	98
11	275	4.9760	.6963E-01	257	.5647	102
12	289	4.9783	.8719E-01	257	.5594	104
13	303	4.9824	.8999E-01	-89	.5583	105
14	317	4.9857	.1097	-88	.5903	107
15	332	4.9900	.1352	-81	.5897	108
16	347	4.9943	.1701	-80	.5888	107
17	362	4.9969	.1895	265	.6422	106
18	377	5.0019	.1992	252	.7156	105
19	392	5.0051	.2225	247	.8101	103
20	407	5.0103	.2097	246	.8468	104
21	422	5.0158	.1811	259	.8582	106
22	437	5.0205	.1736	260	.8671	110
23	452	5.0262	.1566	235	.8714	112
24	467	5.0329	.1845	225	.8815	113
25	482	5.0375	.2286	219	.9043	115
26	497	5.0417	.2255	213	.9519	117
27	511	5.0455	.2293	206	.9856	118
28	525	5.0481	.2185	195	1.020	119
29	539	5.0525	.3051	178	1.040	119
30	553	5.0559	.3177	173	1.003	119
31	567	5.0577	.3548	163	1.032	121
32	581	5.0588	.3610	164	1.042	124
33	595	5.0567	.3705	167	1.085	126
34	609	5.0548	.3700	169	1.185	128
35	623	5.0478	.3232	177	1.271	129
36	637	5.0330	.2734	182	1.334	132
37	651	5.0029	.2779	173	1.379	-43
38	665	4.9427	.2187	154	1.439	-38
39	679	4.8118	.2020	-13	1.579	-33
40	693	4.5685	.8687	-31	1.864	-28

References

1. J.H. Ormrod, C.B. Bigham, K.C. Chan, E.A. Heighway, C.R. Hoffmann, J.A. Hulbert, H.R. Schneider and Q.A. Walker, Trans. IEEE NS-26, 2034 (1979).

2. C.B. Bigham, Nucl. Inst. & Methods 131, 223 (1975). E.A. Heighway, Trans. IEEE NS-24, 1479 (1977).

3. E.A. Heighway, to be published.

4. M.D. Thompson, Los Alamos Report LA-5304-MA (1973).

5. S.W. Mosko, E.D. Hudson, R.S. Lord, D.C. Hensley and J.S. Biggerstaff, Proc. IEEE NS-24, 1269 (1977).

6. S.W. Mosko, private communication.

7. W. Busse and H. Kluge, 7th Int. Conf. on Cyclotrons, Zurich, 1975, Birkhausser, p. 557.

8. E.A. Heighway and K.R. Chaplin, Atomic Energy of Canada Limited, Report AECL-6079 (1977).

9. The closing of the midplane gap exceeded by $\sim$ 80% the calculated deflection (Q.A. Walker, private communication). The calculation assumed perfect mating faces between the pole, upper end ring and yoke wall; the greater deflection is partly attributed to springing at these machined surfaces.

10. J.I. Budnick, L.J. Bruner, R.J. Blume and E.L. Boyd, J. Appl. Phys. 32, 1205 (1961).

ISSN 0067 - 0367

To identify individual documents in the series we have assigned an AECL- number to each.

Please refer to the AECL- number when requesting additional copies of this document

from

Scientific Document Distribution Office
Atomic Energy of Canada Limited
Chalk River, Ontario, Canada
K0J 1J0

Price $3.00 per copy

ISSN 0067 - 0367

Pour identifier les rapports individuels faisant partie de cette série nous avons assigné un numéro AECL- à chacun.

Veuillez faire mention du numéro AECL- si vous demandez d'autres exemplaires de ce rapport

au

Service de Distribution des Documents Officiels
L'Energie Atomique du Canada Limitée
Chalk River, Ontario, Canada
K0J 1J0

Prix $3.00 par exemplaire

3015–80